Journal of The Electrochemical Society

OPEN ACCESS

The Electrochemical Detection of 4-chloro-2-methylphenoxyacetic Acid (MCPA) Using a Simple Activated Glassy Carbon Electrode

To cite this article: Tian Yu *et al* 2022 *J. Electrochem. Soc.* **169** 037514

Journal of The Electrochemical Society, 2022 **169** 037514

The Electrochemical Detection of 4-chloro-2-methylphenoxyacetic Acid (MCPA) Using a Simple Activated Glassy Carbon Electrode

Tian Yu, Orla Fenelon, Karen M. Herdman, and Carmel B. Breslin[z]

Department of Chemistry, Maynooth University, Maynooth, Co. Kildare, Ireland

4-Chloro-2-methylphenoxyacetic acid (MCPA) is one of the pesticides most widely used to control broadleaf weeds in arable and horticultural crops and it leaches readily into groundwater bodies causing pollution. In this study, a sensor was fabricated by the simple activation of a glassy carbon electrode (GCE) in an aqueous phosphate solution by cycling the GCE between –2.0 and 2.4 V vs SCE. The activated GCE exhibited very good detection of MCPA, with a linear concentration range extending from 1 to 850 μM (cyclic voltammetry) and a limit of detection (LOD) of 0.008 μM, which was obtained using differential pulse voltammetry. A more thermodynamically favoured oxidation of MCPA was observed at the activated GCE, with an approximate shift of 110 mV in the peak potential to lower potentials. Very good reproducibility and stability were achieved, with the sensor giving similar peak currents over a 30-day immersion period. Good selectivity was achieved in the presence of nitrates, nitrites, sulfates and structurally related compounds such as nitro-phenols. The promising performance of the activated GCE in the sensing of MCPA was attributed to the generation of oxygenated functional groups and an increased surface area arising from the local dissolution of the GCE during activation.

 [DOI: 10.1149/1945-7111/ac5c03]

Manuscript received October 31, 2021. Published March 21, 2022. *This paper is part of the JES Focus Issue on Women in Electrochemistry.*

Throughout the world, pesticides and herbicides have increasingly become a fundamental part of modern agriculture and sustainable food supply.[1] However, these chemical substances, which have the ability to kill a variety of pests, are contaminating natural ecosystems and threatening biodiversity.[2] Pesticides are broadly divided into fungicides, insecticides, rodenticides and herbicides[3] and one of the more widely utilised herbicides is 4-chloro-2-methylphenoxyacetic acid (MCPA). MCPA is employed in agriculture, especially in marginal and upland agricultural areas as it is very effective in weed control.[4] It is normally applied through spraying and therefore it is frequently found in plants, soil and water[5,6] leading to significant environmental pollution.[7] Additionally, due to its relatively good solubility in water and rather poor adsorption by the soil substrate, MCPA enters surface and ground water bodies.[8] Indeed, MCPA has been found in several water systems, including rivers and streams, during various water quality surveillance programmes.[8,9] MCPA is harmful to aquatic species,[10] animals[11] and can impact on human health even at relatively low concentrations.[12] Therefore, the development of rapid, sensitive and simple MCPA detection methods is urgently required not only for human health and the environment, but also for providing data on the removal efficiency of MCPA and other pesticides from aquatic environments.

So far, several MCPA detection methods have been developed and these include high performance liquid chromatography (HPLC),[13] capillary electrophoresis,[14] solid phase extraction coupled with ion mobility spectrometry,[15] electrochemiluminescence[16] and chemiluminescence.[17] However, these methods suffer from expensive equipment, the requirement for trained technical personnel, complex sample preparation and time-consuming analyses. Comparatively, electrochemical sensors exhibit unique advantages, such as being rapid, reliable, cost-effective and can be easily transported to various water bodies to give onsite and real-time detection.

Nevertheless, there are very few electrochemical-based sensors that have been developed and reported for the determination of MCPA. On searching the literature only three papers reported by Brett and co-workers[18,19] and Bialek et al.[20] were found. In these studies, Brett and co-workers combined β-CD with multi-walled carbon nanotubes (MWCNTs) and this dispersion was then applied to a polyaniline modified GCE electrode to give PANI-β-CD/MWCNT/GCE. The sensor was shown to give a linear range from 10 to 100 μM with a detection limit of 0.99 μM for MCPA.[18] In a related study, the same group employed the PANI-β-CD/MWCNT/GCE sensor for the simultaneous detection of MCPA and its metabolite, 4-chloro-2-methylphenol.[19] The authors attributed the enhanced oxidation peak currents observed for MCPA to both the MWCNTs and β-CD. Bialek et al.[20] employed a carbon paste electrode modified with mesoporous silica or powdered activated carbon and found a linear range between 10 and 500 μM.

It has been shown that the oxidation of carbon-based substrates occurs when polarised to high potentials and this has been reported with carbon nanotubes,[21] activated carbon[22] and glassy carbon electrodes.[23] At these high potentials, which are typically beyond the oxygen evolution reaction, $OH^{\cdot}$ radicals are produced which can attack the C–C bonds giving rise to the formation of oxygen-containing groups.[24] These oxygenated groups have been shown to increase the rate of the electron transfer process and enhance the electrochemical properties of the activated electrode.[23–26] In this paper, a glassy carbon electrode was activated in a slightly acidic phosphate buffer solution, by cycling the electrode in a wide electrochemical window, facilitating both oxidation and reduction processes. This simple activated electrode was then employed in the electrochemical detection of MCPA, to give impressive detection with a wide linear range, a low detection limit and good selectivity.

Experimental Method

All chemicals were obtained from Sigma–Aldrich and were of analytical grade reagents and used without any further purification. The electrochemical measurements, including cyclic voltammetry (CV) and differential pulse voltammetry (DPV), were recorded with a Solartron 1287 or CHI 760 C potentiostat. Electrochemical impedance spectroscopy measurements were carried out using a Solartron 1287 potentiostat coupled with a 1255 FRA (Solartron). The surface morphology was studied using scanning electron microscopy (SEM) with a Hitachi S-3200-N microscope containing a tungsten filament electron source.

A standard three-electrode cell was employed, comprising a glassy carbon electrode (GCE) as the working electrode, a high surface area platinum wire as the counter electrode, and a saturated calomel electrode (SCE) served as the reference. The GCE (3 mm in diameter) was polished with progressively smaller sized diamond suspensions (Akasol) with a final 1 μm particle size, on a micro-cloth (Aka-Napel cloth) to give a mirror finish. Finally, the polished

[z]E-mail: Carmel.Breslin@mu.ie

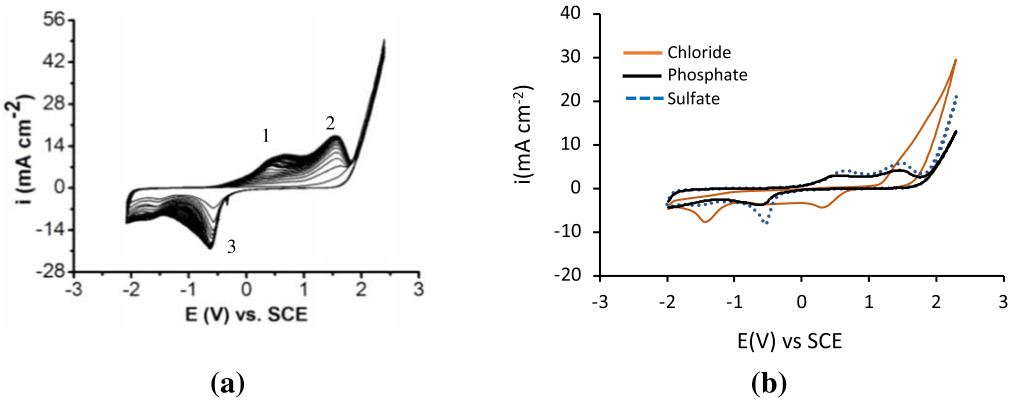

Figure 1. CVs recorded at 100 mV s^{-1} between the potential limits of –2.0 and 2.4 V vs SCE in slightly acidified pH 5.3 solutions during the activation of GCE in (a) 0.05 M phosphate, showing 30 cycles (b) 10th cycle in 0.05 M phosphate, 0.05 M sulfate and 0.05 M chloride.

GCE was sonicated and thoroughly rinsed with deionised water. Unless otherwise stated, the activated GCE was formed in a 0.05 M phosphate buffer by cycling the polished GCE between –2.0 V and 2.4 V vs SCE at 100 mV s^{-1} for 30 cycles. The resulting surfaces were thoroughly rinsed with deionised water and then employed in the electrochemical detection of MCPA in a 0.1 M phosphate buffer solution adjusted to a pH of 5.3.

Two procedures were used in the MCPA electrochemical studies; firstly, the data were recorded using a freshly prepared GCE and secondly the data were recorded in the steady state. For these latter experiments, the activated GCE was cycled until steady state voltammograms were achieved, usually 30 cycles. The CV experiments were performed at a scan rate of 100 mV s^{-1}, unless otherwise stated. DPV measurements were recorded using a pulse amplitude of 50 mV, pulse width of 0.05 s, sampling width of 0.0167 s, a pulse period of 0.50 s, and an increment of 4 mV. The impedance data were recorded at a fixed potential from 1.1 to 1.5 V vs SCE in 0.1 M phosphate buffer using a perturbation potential of 10 mV. All data were recorded after a 3-hr polarisation period to ensure steady state conditions were achieved. The collected data were fitted to an equivalent circuit, keeping the errors below 2%. The long-term stability of the activated GCE was monitored by initially cycling the electrode to give steady-state voltammograms, then the electrode was stored in a 0.1 M phosphate buffer solution and removed at different time intervals and the voltammograms were recorded again and compared with the initial data.

Results and Discussion

Preparation and optimisation of the activated electrodes.—The GCE surface was activated in a slightly acidified phosphate buffered solution by cycling between the potential limits of –2.0 to 2.4 V vs SCE. Typical data are shown in Fig. 1a, where the voltammograms are presented, showing cycles 1 to 30 for the phosphate system. Clear oxidation waves are seen at about 0.70 V (peak 1) and 1.5 V vs SCE (peak 2), while a sharp reduction wave is evident at about –0.60 V vs SCE and a smaller less defined reduction wave emerges at about –1.9 V vs SCE. The peak potential remains essentially constant with increasing cycling for peak 3, however there is a considerable shift in the peak potential for peak 2, increasing from about 0.45 V for the initial cycles to about 0.70 V vs SCE for cycle 30. In all cases the peak currents increase with cycling and this appears to be related to the degree of oxidation with the sharp peak at about –0.6 V vs SCE connected with the reduction of oxides formed at the higher potentials. The influence of the anion is evident in Fig. 1b, where the voltammograms are compared for chloride, phosphate and sulfate anions. Clearly, the anion has a significant influence. The sulfate and phosphate systems are similar, however the voltammograms are very different in the presence of chloride anions. The onset of the oxygen evolution reaction occurs at a much lower overpotential, and the characteristic oxidation waves seen in the vicinity of 0.7 and 1.5 V vs SCE are no longer evident, Fig. 1b. In this case, the Cl^- ions can combine with the $OH^{\cdot}$ species generated during the evolution of oxygen to give various reactive chloride intermediates,[27] such as $ClOH^{\cdot-}$, and these have the potential to alter the activation process.

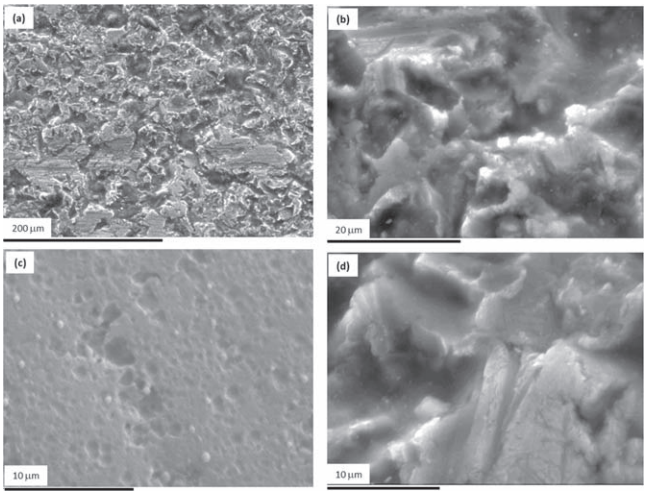

Figure 2. SEM micrographs recorded following cycling of the GCE electrode between –2.0 and 2.4 V vs SCE for 30 cycles at 100 mV s^{-1} in (a) phosphate (b) phosphate at a higher magnification (c) chloride and (d) sulfate.

Typical scanning electron micrographs, illustrating the morphology of the GCE activated in phosphate, chloride and sulfate, are shown in Fig. 2. An etched-like surface is seen with the phosphate system, Figs. 2a and 2b. This etching is consistent with a report by Yi et al.[28] where etching was explained in terms of the degradation of GCE by ring opening of the graphitic structure and the formation of oxides. A similar morphology is seen with the sulfate activated GCE, Fig. 2d, while the morphology of the chloride activated GCE is very different, with the formation of a porous lace-like film.

The freshly prepared activated GCE was initially used to detect MCPA at a relatively high concentration of 4 mM using cyclic voltammetry. As shown in Scheme 1, this oxidation reaction proceeds irreversibly with the transfer of one electron and one proton to yield 4-chloro-2-methylphenol. In Fig. 3a, the voltammograms recorded for the phosphate activated GCE and the unmodified GCE are compared. It is immediately evident that the activated electrode facilitates the oxidation of MCPA as the peak current is considerably higher at 9.01 mA cm^{-2} compared to a much lower peak current of 1.21 mA cm^{-2} for the GCE. It is also evident from

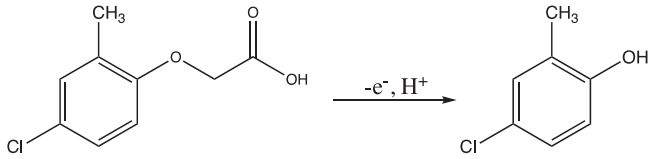

Scheme 1. The structure of MCPA and its electrochemical oxidation to 4-chloro-2-methylphenol.

these voltammograms that activation gives rise to a much higher capacitive current, and this is probably connected with the etched surface, as illustrated in Figs. 2a and 2b. As illustrated in Fig. 3b, the anion in the activation solution has a considerable influence on the electrochemical oxidation of MCPA, with poor detection observed in the presence of chloride and acetate anions. On the other hand, good detection is seen with the sulfate system.

In order to further optimise the performance of the activated GCE in the electrochemical detection of MCPA, the experimental parameters employed in the fabrication of the activated GCE were investigated, including the applied potential ranges, the number of cycles employed in the formation of activated GCE and the pH of the activating solution. The optimum detection of MCPA was observed with the phosphate solution adjusted to a pH of 5.3. Slightly lower peak currents were observed on activation in neutral solutions and also in more acidic solutions. The effects of the activation window and number of cycles are summarised in Figs. 3c and 3d, respectively. Using these studies the optimum activation conditions for the electrochemical oxidation of MCPA were identified as cycling between –2.0 and 2.4 V vs SCE, for 30 cycles in a 0.05 M phosphate buffer adjusted to a pH of 5.3.

Information on the conducting properties of the optimised activated GCE was obtained using electrochemical impedance spectroscopy. The data were recorded at different applied potentials and representative plots are shown in Fig. 4. The impedance data were fitted to the equivalent circuit shown in the inset in Fig. 4a, where R1 represents the solution resistance, R2 corresponds to the charge transfer resistance and CPE1 is a constant phase element. The complex impedance of the CPE is given in Eq. 1, which is a generalised expression corresponding to a resistor with $n = 0$, to a capacitor for $n = 1$, and to an inductor with $n = -1$. In this case it was used to represent a non-ideal capacitor, with $0.8 \leqslant n < 1$.

$$Z_{CPE} = \frac{1}{\omega^n \mathrm{A}} e^{-i\frac{\pi}{2}n} \quad [1]$$

Representative impedance data are presented in Fig. 4a, where the complex plane plots of the GCE and activated GCE electrodes are compared. These data were recorded following a 180 min polarisation period at 1.2 V vs SCE to coincide with the potentials required to oxidise MCPA. It is clear from this analysis that similar data are obtained for both electrodes. Semicircles are seen and there is no evidence of any additional resistance or diffusion paths for the activated GCE. This observation indicates that the modified and bare electrodes are similar and even at these relatively high potentials the systems are well behaved, with the activated GCE exhibiting a somewhat more conducting surface. At 1.2 V vs SCE, where oxidation of MCPA is observed in the cyclic voltammograms, the charge transfer resistance was estimated at 2.9 kΩ cm^2 for the activated GCE and 120.6 kΩ cm^2 for the GCE electrode, clearly illustrating the good conducting properties of the activated GCE. The constant phase elements with n values of 0.83 represent

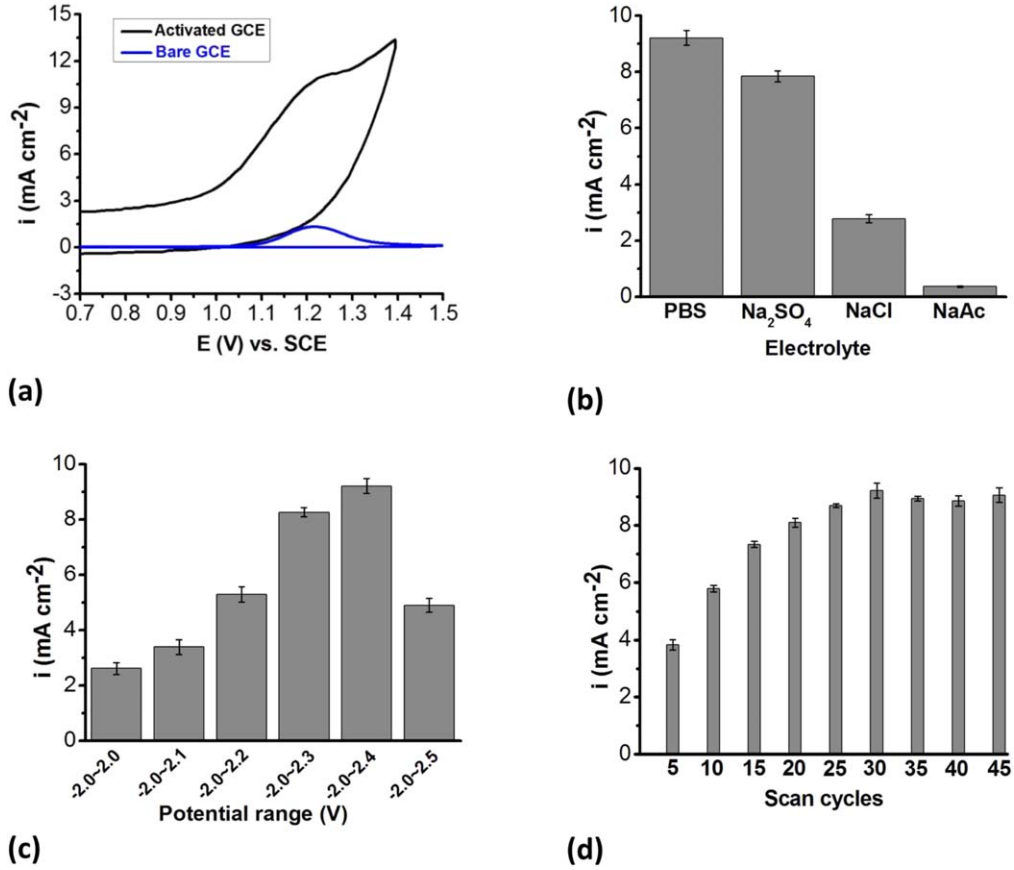

Figure 3. (a) CVs recorded using GCE (blue) and activated GCE (black), (b) Peak current recorded in MCPA for activated GCE formed in different electrolytes , and MCPA peak current as a function of (c) activation window and (d) activation cycles. All CVs performed at 100 mV s^{-1} in 4.0 mM MCPA in phosphate buffer, second cycle data used.

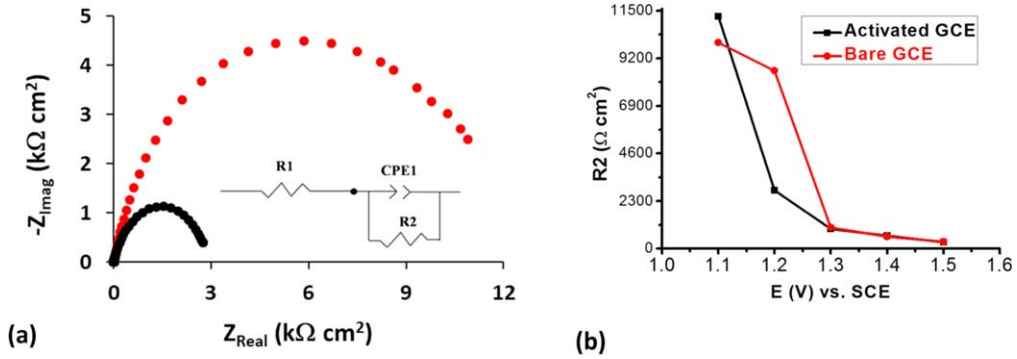

Figure 4. (a) The electrochemical impedance spectra for bare GCE (red) and activated GCE (black) recorded in phosphate buffer at 1.2 V vs SCE, (b) Charge transfer resistance (R2) plotted as a function of the applied potential for bare (red) and activated GCE (black).

Table I. Reproducibility of the activated GCE in the detection of 4.0 mM MCPA.

	Peak Current (mA cm^{-2})					RSD (%)
	1	2	3	4	5	(n = 5)
Freshly prepared activated GCE	9.017	9.756	8.956	8.057	9.831	0.57
	Peak Current (mA cm^{-2})			RSD (%)		
	1	2	3	4	5	(n = 5)
Activated GCE in the steady state	1.219	1.217	1.218	1.220	1.222	0.19

non-ideal capacitors, and interestingly, this value was higher for the activated GCE (8.43×10^{-4} Ω^{-1} $s^{0.83}$ for activated GCE and 3.37×10^{-4} Ω^{-1} $s^{0.83}$ for GCE). This higher capacitance is consistent with the etched surface, Figs. 2a and 2b, and the high capacitive currents observed in Fig. 3a. In Fig. 4b, the charge-transfer resistance, R2, is plotted as a function of the applied potential, again indicating that the activated GCE remains conducting at these high potentials. The lower charge-transfer resistance values observed in the vicinity of 1.3 V to 1.5 V vs SCE are related to the oxygen evolution reaction, which gives nearly identical values for both electrodes. Furthermore, the stability of the activated GCE was monitored by measuring the impedance over a 24-h period. Nearly identical data were recorded from 3 h to 24 h, indicating very good stability at these relatively high potentials.

Oxidation of MCPA at the activated GCE.—Steady-state conditions were employed in the electrochemical characterisation studies. In this case, the freshly modified and optimised activated GCE was firstly cycled between –0.1 V and 1.5 V vs SCE in the MCPA or phosphate buffer solution for 30 cycles to achieve steady state conditions. Although, the oxidation waves for MCPA decreased in intensity with increasing cycling before the steady state conditions were achieved, greater reproducibility was achieved under steady state conditions and this is illustrated in Table I. It is clear from this table that although the steady state conditions give lower peak currents, improved reproducibility is achieved with the RDS at 0.19% for steady state compared with 0.57% for the freshly prepared sensors. Moreover, the high capacitive currents, observed in Fig. 3a, are reduced considerably with repeated cycling to give a low background current.

The influence of the solution pH on the electrochemical detection of MCPA was investigated between a pH of 2.5 and 8.3. Representative DPVs are shown in Fig. 5, where it is clear that both the peak current and peak potential depend on the pH of the solution. It is evident from Fig. 5a that the highest peak current is observed in the slightly acidic solution with a pH of 5.3. As the pH is increased further the peak current decreases and this is consistent with the participation of H^+ ions in the oxidation reaction, Scheme 1. The p*K*a of MCPA is about 3.07 (reported typically between 3.05 and 3.13),[29] indicating that the MCPA becomes more neutral as the solution becomes more acidic, with the neutral MCPA existing at a pH of 3.0. This neutral form will be less soluble in

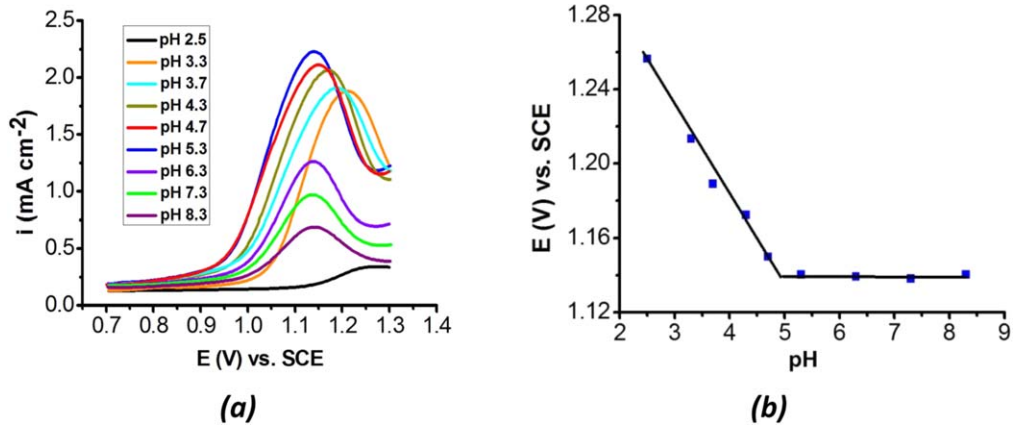

Figure 5. (a) DPV voltammograms recorded in 4.0 mM MCPA in a phosphate buffer solution at different pH values and (b) peak potential, Ep, plotted as a function of pH.

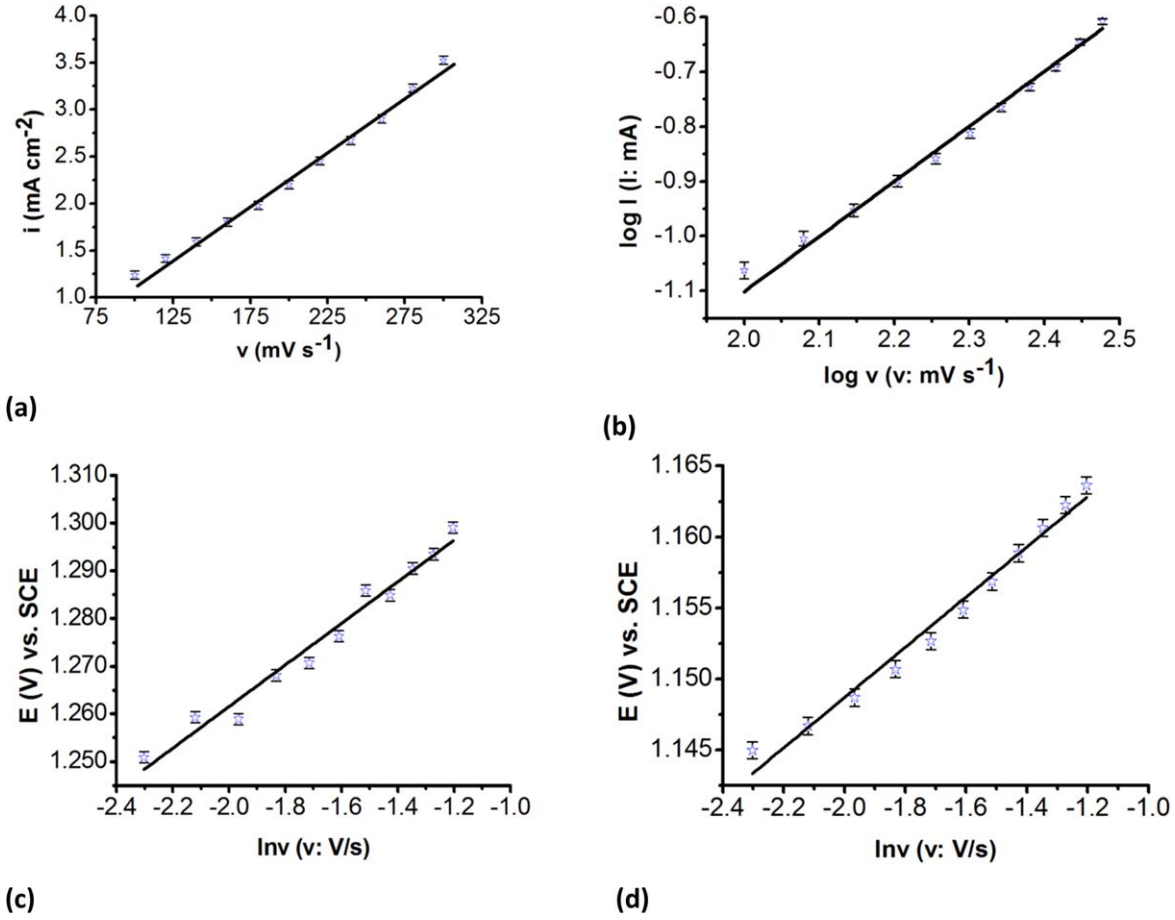

Figure 6. (a) Steady state peak oxidation currents vs the scan rates for activated GCE, (b) logarithm of steady state peak oxidation currents vs logarithm of scan rates for the activated GCE and peak potentials as a function of the logarithm of scan rate for (c) bare GCE and (d) activated GCE.

aqueous solution and this is probably connected with the particularly low peak current observed at a pH of 2.5. On plotting the peak potential as a function of the solution pH, a linear trend was observed between a pH of 2.5 and about 5.0, as shown in Fig. 5b. The regression equation was obtained as, $Ep = -0.048\ \text{pH} + 1.37$. On comparing this computed slope with the theoretical slope of 0.059 *m*/*n*, where *m* represents the number of protons transferred and *n* corresponds to the number of electrons transferred, the *m*/*n* value was estimated as 1.22 and this is consistent with the transfer of equal numbers of protons and electrons, as illustrated in Scheme 1.

In order to determine if the oxidation of MCPA was under diffusion or adsorption control, the peak currents were recorded as a function of the scan rate after cycling the activated GCE in 4.0 mM MCPA to achieve steady state. On plotting the peak current as a function of the scan rate, a linear plot was obtained, as illustrated in Fig. 6a ($R^2 = 0.998$), indicating that the oxidation of MCPA is an absorption-controlled process. Furthermore the slope of the plot in Fig. 6b, where the logarithm of the current is plotted as a function of the logarithm of the scan rate, is 1.0, which is again consistent with an adsorption-controlled process.

Using the relationship in Eq. 2, where E_p represents the peak potential, $E_{p/2}$ is the half-wave potential, *n* is the number of electrons transferred and α is the charge-transfer coefficient, the $E_p - E_{p/2}$ value was computed as 98.4 mV for the un-modified GCE and 78.0 mV for the activated GCE system. Taking $n = 1$, the α value was computed as 0.60 for the activated GCE system, which is close to the value of 0.55, which is normally taken as a representative α value.

$$E_p - E_{p/2}(\text{mV}) = (47.7/\alpha n) \quad [2]$$

On comparing Figs. 6c and 6d, it is obvious that there is a clear shift in the peak potential (E_p) of about 110 mV from 1.25 V vs SCE for GCE to 1.14 V vs SCE for the activated electrode, indicating a more thermodynamically viable oxidation reaction. In both cases, linear relationships between the peak potential and logarithm of the scan rate are observed. The linear regression equations were found as $Ep = 0.025\ \ln\upsilon + 1.24$ ($R^2 = 0.980$) (for the activated GCE under steady state conditions, $Ep = 0.046\ \ln\upsilon + 1.40$ ($R^2 = 0.969$) for the unmodified GCE and $Ep = 0.0411\ \ln\upsilon + 1.30$ ($R^2 = 0.695$) (not shown) for the freshly prepared activated GCE. The slope of the linear plot can be expressed by Eq. 3, in accordance with the Laviron equation[30] where *R* and *F* are the universal constants and *T* represents the thermodynamic temperature. Using this relationship, the αn value was computed as 0.55, 0.62 and 1.0 for the unmodified GCE, freshly prepared activated GCE and the activated GCE in steady state conditions. Applying the α value of 0.55 (for irreversible electrochemical reactions), the number of electrons involved in the electrochemical oxidation of MCPA was estimated as 1.0, 1.1 and 1.8 respectively, for the GCE, freshly activated GCE and steady state activated GCE. The values obtained for the unmodified GCE, and freshly activated GCE are in very good agreement with Scheme 1, however the slope of 0.0205 V deviates considerably from the ideal value of 0.0514 V for the activated GCE under steady state conditions.

$$E_{pc}/\log u = 2.3RT/\alpha nF \quad [3]$$

Electrochemical detection of MCPA and performance of the activated GCE sensor.—The performance of the activated GCE in the electrochemical detection of MCPA was studied using a combination of CV and DPV measurements. The activated GCE

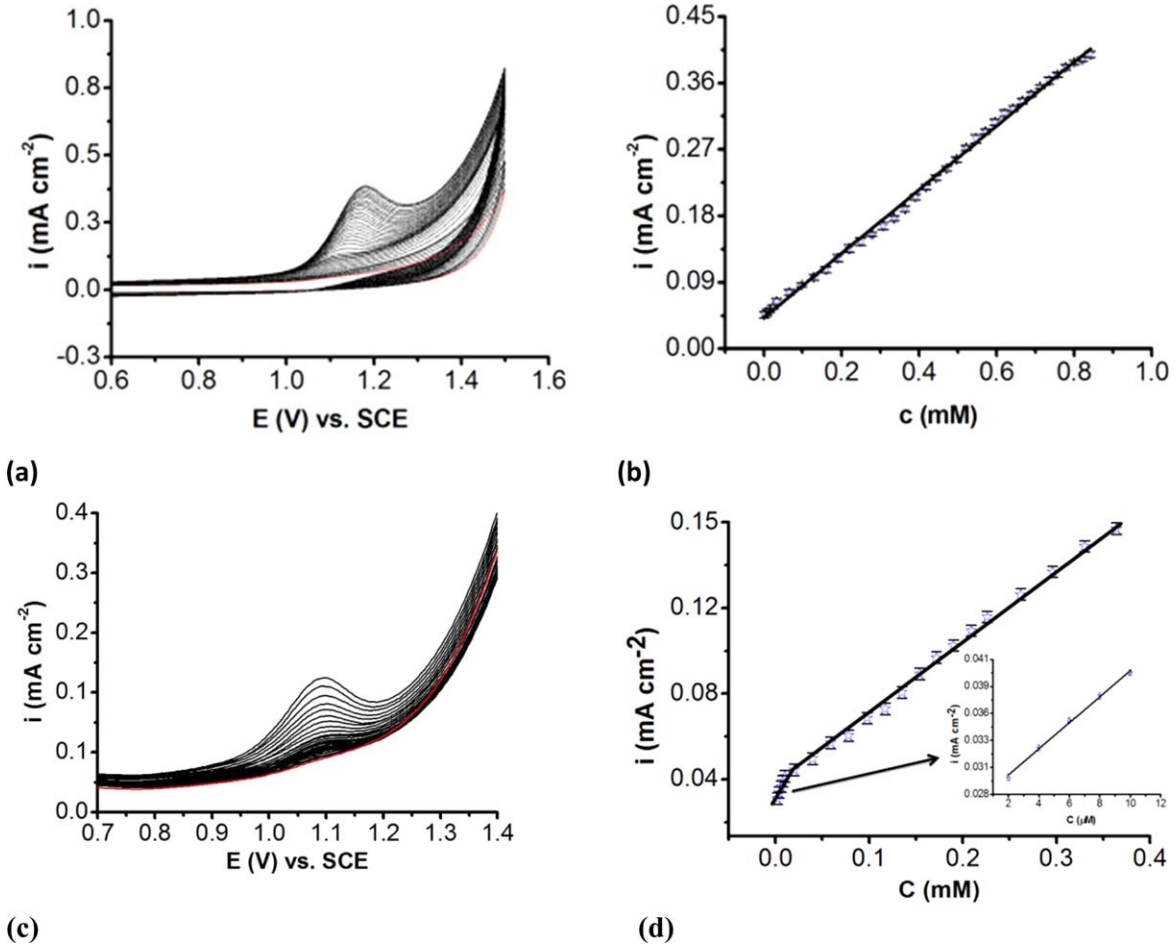

Figure 7. (a) Steady-state CVs recorded at 100 mV s^{-1} for MCPA at concentrations from 1 to 850 μM, (b) peak current as a function of the MCPA concentration, (c) steady-state DPVs of MCPA at concentrations from 2 to 365 μM, (d) peak currents as a function of MPCA concentration, the inset shows the concentration range from 2 to 10 μM (red curve recorded in phosphate solution).

was cycled for 30 cycles in the phosphate buffer solution and then aliquots of MCPA were added and the voltammograms were recorded. The resulting voltammograms are presented in Fig. 7a where it is evident that the peak oxidation currents increase with increasing concentration. These peak currents were plotted as a function of the MCPA concentration, and these data are shown in Fig. 7b. Excellent linearity was achieved with an R^2 value of 0.998 and the linear regression equation was deduced as, $i = 0.4322$ [MCPA] + 0.0427, where the concentration of MCPA was expressed in mM and i in mA cm^{-2}. Moreover, very good reproducibility was achieved, as indicated by the error bars.

The linear region extends over a considerable concentration range, extending from 1 to 850 μM, as illustrated in Fig. 7b. The detection limit (LOD) was calculated to be 0.02 μM, based on Eq. 4, where S_b is the standard deviation of the base line and m is the sensitivity, or slope, of the linear calibration plot. Similarly, the DPV technique was employed to detect MCPA. These voltammograms are displayed in Fig. 7c, while two linear regions are depicted in Fig. 7d. Again, excellent linearity was observed at the low concentration range from 2 to 10 μM, with the linear regression equation, $i = 0.978$[MCPA] + 0.064 and an R^2 values of 0.993 (concentration of MCPA given as mM and i in units of mA cm^{-2}). The detection limit was calculated as 0.008 μM.

$$LOD = \frac{3S_b}{m} \quad [4]$$

The sensing performance of the activated GCE sensor is compared with previously developed sensors for MCPA and 4-(2,4 dichlorophenoxy)butyric acid, as shown in Table II. It is clearly evident from this analysis that the simple activated GCE sensor compares very well with these previous studies, giving a wider linear range and lower LOD values.

Another important and significance element in the fabrication of a sensor is selectivity. For these studies, a number of water contaminants, such as nitrates, nitrites, sulfates, Cu(II) ions and tetramethylammonium chloride (TBACl), a widely used industrial chemical, which has also been used as a low-residue bactericide, were employed. These salts were added to the MCPA-containing solution and then the CVs were recorded in the interference-containing solutions and compared with the data obtained in the absence of the interferents. The level of interference was measured using the relative current intensity, I/I_0, where I_0 refers to the MCPA peak current in the absence of the interferent and I is the corresponding peak current measured in the presence of the interferent. This study is summarised in Fig. 8a, where the interferent concentrations were set at 9.4 mM for $NaNO_3$, 11.6 mM for $NaNO_2$, 5.0 mM $CuSO_4$ and 3.0 mM for TBACl, giving equal mass ratios of 1:1 for MCPA and the interferent. It can be observed that there is no significant interference observed for these contaminants, the reproducibility is good, as evidenced from the error bars and the difference between the pure MCPA and the interferent containing MCPA solutions is well below 5%.

However, none of these contaminants are structurally related to MCPA and therefore additional structurally related contaminants were selected. The structurally related interferences include 3.2 mM 2,4-DB (4-(2,4-dichlorophenoxy) butyric acid), 5.8 mM o-NP (4-nitrophenol), 5.8 mM p-NP (2-nitrophenol) and 5.6 mM 4-Cl-2MP

Table II. Performance of MCPA electrochemical based sensors.

System	LOD/μM	Linear region/μM	References
PANi/CNT/β-CD	1.1	10–50	19
PANi/CNT/β-CD	0.99	10–100	18
Powdered activated carbon (Norit SX-2) paste	0.7	10–500	20
Mesoporous silica SBA-15 carbon paste	1.3	10–500	20
[a)]Co-porphyrin/molecularly imprinted polymer	40	200–2000	31
Activated/GCE	0.02 (CV) 0.008 (DPV)	1–850	This work

a) Employed in the detection of 4-(2,4 dichlorophenoxy)butyric acid.

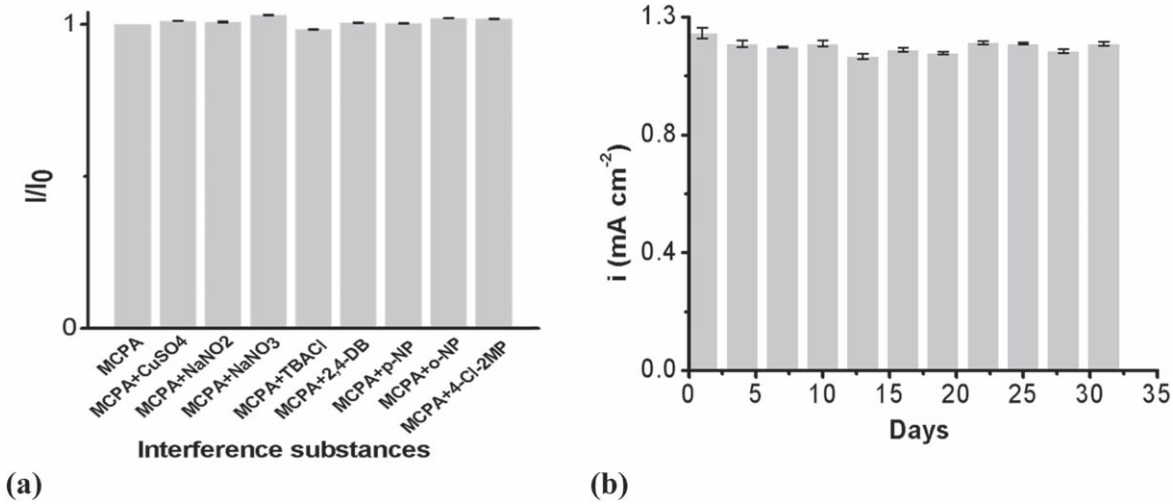

Figure 8. (a) Normalised oxidation peak currents of MCPA vs the eight interfering substances with a mass ratio of 1:1; (b) the stability study of the activated GCE over 30 days in 4.0 mM MCPA solution.

(4-chloro-2-methyl phenol). These all have phenol rings like MCPA, and these compounds are also electroactive. Although the oxidation/reduction of these compounds was indeed observed at the activated GCE (data not shown) the redox waves were seen at lower potentials compared with MCPA, giving no significant interference with the detection of MCPA. This good selectivity may be due to hydrogen bonding between the carboxylic group of the MCPA molecule and the oxygenated groups, such as OH, which are generated during the activation of the GCE.

Reproducibility and stability are equally important factors in the performance of a sensor. For the reproducibility tests, the activated GCE was cycled for 30 cycles in the MCPA solution to achieve steady state conditions and then the activated GCE was used to determine MCPA in five consecutive experiments, with washing with deionised water between each test (results are summarised in Table I). In addition, the stability of the activated GCE in the steady state was monitored in the phosphate solution over 30 days, and these data are illustrated in Fig. 8b. At different time intervals, the sensor was removed from the phosphate solution and transferred to the MCPA solution and the voltammograms were recorded. Then the electrode was thoroughly rinsed with distilled water and transferred to the storage solution. This was repeated several times to give the data in Fig. 8b. While there is some variation over the 30-day period, there is no evidence of any significant loss in the sensing ability of the activated GCE, with the standard deviations in the peak currents $< 5\%$. This observation demonstrates clearly that the simple activated GCE has very good stability under steady-state conditions.

Electrochemical detection of MCPA metabolite.—The activated GCE can also be used in the electrochemical detection of the MCPA metabolite. As shown in the voltammograms in Fig. 3, the oxidation of MCPA gives an irreversible electrochemical reaction with a broad oxidation wave. This oxidation reaction leads to the production of 4-chloro-2-methylphenol, as illustrated in Scheme 1. On extending the electrochemical window to lower applied potentials the electrochemical behaviour of this product molecule was observed and this is illustrated in Fig. 9a. The emergence of redox waves in the vicinity of –0.10 V to 0.15 V vs SCE becomes evident. As shown in Fig. 9a the broad reduction wave, labelled as Peak 1 depends on the concentration of MCPA, increasing in magnitude as the concentration of MCPA is increased. The reduction of 4-chloro-2-methylphenol has previously been described by Scheme 2.[19] Interestingly, this reduction wave was not seen at the unmodified GCE electrode, while it is clearly evident at the activated GCE at relatively low concentrations of 0.14 mM for MCPA. Moreover, Bialek et al.,[20] observed only a single irreversible oxidation wave, corresponding to the oxidation of MCPA, on cycling a modified carbon paste electrode between the potential limits of 0.0 and 1.5 V, suggesting that the emergence of this reduction wave is connected with the oxygenated species formed during the activation of the GCE.

In order to confirm this assignment, 4-chloro-2-methylphenol was employed as the analyte. The freshly prepared activated GCE was cycled in the 4-chloro-2-methylphenol (4-Cl-2MP) containing solutions and the corresponding voltammograms, which were recorded at different concentrations, are presented in Fig. 9c. Clearly, peak 1 in Fig. 9a corresponds with the broad reduction wave between 0.0 and –0.1 V vs SCE, evident in Fig. 9c, and this peak is consistent with the reduction reaction outlined in Scheme 2.

The linear calibration curve obtained using steady-state conditions in the 4-chloro-2-methylphenol is shown in Fig. 9d, where the peak current of the reduction wave centred between 0.0 and –0.1 V vs SCE was used. Good linearity is achieved indicating that the activated GCE is an effective sensor for the MCPA metabolite. On further inspecting the voltammograms in Fig. 9c it is clear that these

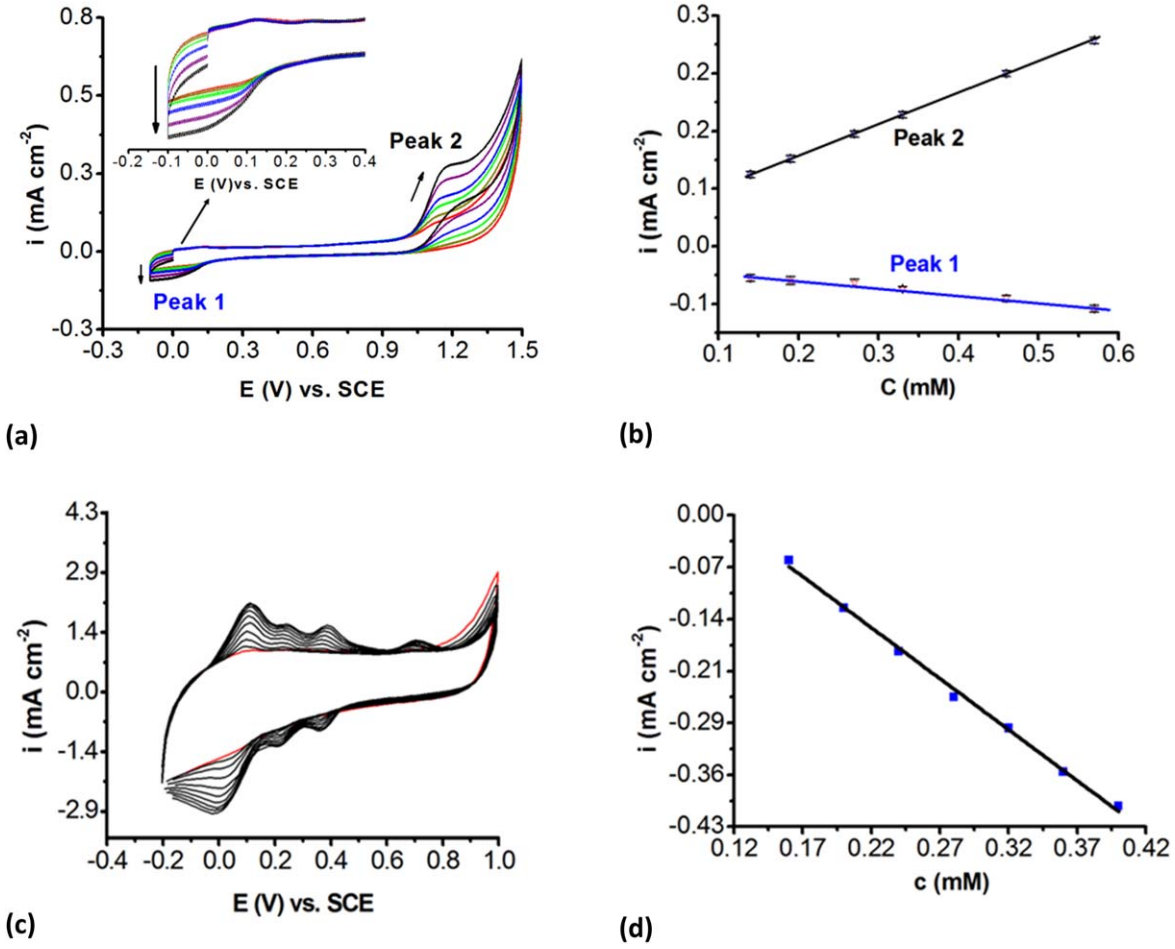

Figure 9. (a) CVs recorded for activated GCE at 100 mV s^{-1} in MCPA at concentrations from 0.14 to 0.57 mM, (b) peak currents plotted as a function of MCPA concentration, (c) CVs recorded for the freshly prepared activated GCE at 100 mV s^{-1} in 4-chloro-2-methylphenol at 0.12, 0.16, 0.20, 0.24, 0.32, 0.36 and 4.0 mM, where the red trace was recorded in phosphate (blank) and (d) calibration curve recorded with activated GCE at steady state conditions in the detection of 4-chloro-2-methylphenol.

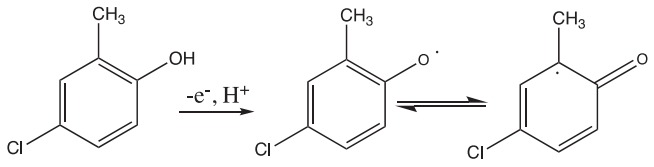

Scheme 2. Reduction of 4-chloro-2-methylphenol as proposed by Rahemi et al.[19]

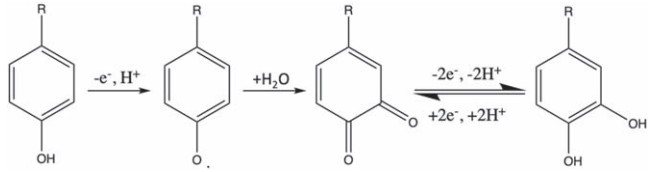

Scheme 3. Electrochemistry of para phenol compounds.

resemble the electrochemistry of phenols.[32] A clear oxidation wave is seen at about 0.10 V vs SCE followed by a quasi-reversible couple in the vicinity of 0.20 V to 0.40 V vs SCE, while an additional oxidation wave is evident at about 0.70 V vs SCE. The quasi-reversible two electron, two proton transfer reaction, associated with the conversion between the quinone and the hydroquinone compounds, Scheme 3, can be assigned to the redox couple at about 0.39 V vs SCE, with a peak separation of 26 mV. The oxidation wave seen at about 0.1 V vs SCE is more difficult to explain, but it appears to be connected with the initial reduction of the MCPA metabolite, Scheme 2.

Conclusions

A new and simple electrochemical sensor for the detection of MCPA was developed by the activation of GCE. Impressive electrochemical detection was achieved, with a wide dynamic linear region, extending from 1 to 850 μM and a LOD value of 0.02 μM obtained using cyclic voltammetry, while the LOD was further reduced to 0.008 μM with DPV. This was accompanied by good reproducibility and stability. It was further observed that 4-chloro-2-methylphenol produced from the oxidation of MCPA was reduced at the activated GCE. This shows that the activated modified electrode can not only be employed in the electrochemical detection of MCPA, but may also be used to follow the degradation efficiency of MCPA by monitoring the 4-chloro-2-methylphenol concentration.

Acknowledgments

The authors would like to acknowledge funding provided by the Irish Research Council, award number GOIPG/2020/657.

ORCID

Carmel B. Breslin https://orcid.org/0000-0002-0586-5375

References

1. J. Pretty, "Intensification for redesigned and sustainable agricultural systems." *Science*, **362**, 6417 (2018).
2. J. Wolfram, S. Stehle, S. Bub, L. L. Petschick, and R. Schulz, "Water quality and ecological risks in European surface waters—monitoring improves while water quality decreases." *Environ. Int.*, **152**, 106479 (2021).
3. C. S. Pundir and A. Malik, "Preety, Bio-sensing of organophosphorus pesticides: a review." *Biosens. Bioelectron.*, **140**, 111348 (2019).
4. P. A. Morton, R. Cassidy, S. Floyd, D. G. Doody, W. C. McRoberts, and P. Jordan, "Approaches to herbicide (MCPA) pollution mitigation in drinking water source catchments using enhanced space and time monitoring." *Sci. Total Environ.*, **755**, 142827 (2021).
5. A. T. K. Tran, R. V. Hyne, and P. Doble, "Determination of commonly used polar herbicides in agricultural drainage waters in Australia by HPLC." *Chemosphere.*, **67**, 944 (2007).
6. T. Paszko, P. Muszyński, M. Materska, M. Bojanowska, M. Kostecka, and I. Jackowska, "Adsorption and degradation of phenoxyalkanoic acid herbicides in soils: A review." *Environ. Toxicol. Chem.*, **35**, 271 (2016).
7. O. Pozo, E. Pitarch, J. V. Sancho, and F. Hernández, "Determination of the herbicide 4-chloro-2-methylphenoxyacetic acid and its main metabolite, 4-chloro-2-methylphenol in water and soil by liquid chromatography-electrospray tandem mass spectrometry." *J. Chromatogr. A*, **923**, 75 (2001).
8. N. E. Glozier et al., "Occurrence of glyphosate and acidic herbicides in select urban rivers and streams in Canada." *Environ. Sci. Pollut. Res.*, **19**, 821 (2012).
9. M. A. Rippy, A. Deletic, J. Black, R. Aryal, J.-L. Lampard, J. Y.-M. Tang, D. McCarthy, P. Kolotelo, J. Sidhu, and W. Gernjak, "Pesticide occurrence and spatio-temporal variability in urban run-off across Australia." *Water Res.*, **115**, 245 (2017).
10. A. Piotrowska, A. Syguda, Ł. Chrzanowski, and H. J. Heipieper, "Toxicity of synthetic herbicides containing 2,4-D and MCPA moieties towards Pseudomonas putida mt-2 and its response at the level of membrane fatty acid composition." *Chemosphere.*, **144**, 107 (2016).
11. K. Wunnapuk, X. Liu, G. C. Gobe, Z. H. Endre, P. W. Peake, J. E. Grice, M. S. Roberts, and N. A. Buckley, "Kidney biomarkers in MCPA-induced acute kidney injury in rats: Reduced clearance enhances early biomarker performance." *Toxicol. Lett.*, **225**, 467 (2014).
12. M. Pahwa, S. A. Harris, K. Hohenadel, J. R. McLaughlin, J. J. Spinelli, P. Pahwa, J. A. Dosman, and A. Blair, "Pesticide use, immunologic conditions, and risk of non-Hodgkin lymphoma in Canadian men in six provinces." *Int. J. Cancer.*, **131**, 2650 (2012).
13. K. Seebunrueng, P. Phosiri, R. Apitanagotinon, and S. Srijaranai, "A new environment-friendly supramolecular solvent-based liquid phase microextraction coupled to high performance liquid chromatography for simultaneous determination of six phenoxy acid herbicides in water and rice samples." *Microchem. J.*, **152**, 104418 (2020).
14. H. Tabani, A. R. Fakhari, A. Shahsavani, M. Behbahani, M. Salarian, A. Bagheri, and S. Nojavan, "Combination of graphene oxide-based solid phase extraction and electro membrane extraction for the preconcentration of chlorophenoxy acid herbicides in environmental samples." *J. Chromatogr. A*, **1300**, 227 (2013).
15. M. Mohammadnejad, Z. Gudarzi, S. Geranmayeh, and V. Mahdavi, "HKUST-1 metal-organic framework for dispersive solid phase extraction of 2-methyl-4-chlorophenoxyacetic acid (MCPA) prior to its determination by ion mobility spectrometry." *Microchim. Acta*, **185**, 495 (2018).
16. Y. Yang, G. Fang, X. Wang, F. Zhang, J. Liu, W. Zheng, and S. Wang, "Electrochemiluminescent graphene quantum dots enhanced by MoS_2 as sensing platform: a novel molecularly imprinted electrochemiluminescence sensor for 2-methyl-4-chlorophenoxyacetic acid assay." *Electrochim. Acta*, **228**, 107 (2017).
17. S. Torres-Cartas, C. Gómez-Benito, and S. Meseguer-Lloret, "FI on-line chemiluminescence reaction for determination of MCPA in water samples." *Anal. Bioanal. Chem.*, **402**, 1289 (2012).
18. V. Rahemi, J. J. Vandamme, J. M. P. J. Garrido, F. Borges, C. M. A. Brett, and E. M. P. J. Garrido, "Enhanced host-guest electrochemical recognition of herbicide MCPA using a β-cyclodextrin carbon nanotube sensor." *Talanta*, **99**, 288 (2012).
19. V. Rahemi, J. M. P. J. Garrido, F. Borges, C. M. A. Brett, and E. M. P. J. Garrido, "Electrochemical sensor for simultaneous determination of herbicide MCPA and its metabolite 4-chloro-2-methylphenol. Application to photodegradation environmental monitoring." *Environ. Sci. Pollut. Res.*, **22**, 4491 (2015).
20. A. Bialek, K. Skrzypczynska, K. Kusmierek, and A. Swiatkowski, "Voltammetric determination of MCPA, 4-chloro-o-cresol and o-cresol in water using a modified carbon paste electrode." *Int. J. Electrochem. Sci.*, **14**, 228 (2019).
21. A. F. Holloway, G. G. Wildgoose, R. G. Compton, L. Shao, and M. L. H. Green, "The influence of edge-plane defects and oxygen-containing surface groups on the voltammetry of acid-treated, annealed and 'super-annealed' multiwalled carbon nanotubes." *J. Solid State Electrochem.*, **12**, 1337 (2008).
22. X. Liu, Y. Wang, L. Zhan, W. Qiao, X. Liang, and L. Ling, "Effect of oxygen-containing functional groups on the impedance behavior of activated carbon-based electric double-layer capacitors." *J. Solid State Electrochem.*, **15**, 413 (2011).
23. D. Huang, Y. Cheng, H. Xu, H. Zhang, L. Sheng, H. Xu, Z. Liu, H. Wu, and S. Fan, "The determination of uric acid in human body fluid samples using glassy carbon electrode activated by a simple electrochemical method." *J. Solid State Electrochem.*, **19**, 435 (2015).
24. A. Rana, N. Baig, and T. A. Saleh, "Electrochemically pretreated carbon electrodes and their electroanalytical applications—a review." *J. Electroanal. Chem.*, **833**, 313 (2019).
25. R. C. Tenent and D. O. Wipf, "Local electron transfer rate measurements on modified and unmodified glassy carbon electrodes." *J. Solid State Electrochem.*, **13**, 583 (2009).
26. B. Healy, F. Rizzuto, M. de Rose, T. Yu, and C. B. Breslin, "Electrochemical determination of acetaminophen at a carbon electrode modified in the presence of β-cyclodextrin: role of the activated glassy carbon and the electropolymerised β-cyclodextrin." *J. Solid State Electrochem.*, **25**, 2599 (2021).
27. A. Farhat, J. Keller, S. Tait, and J. Radjenovic, "Assessment of the impact of chloride on the formation of chlorinated by-products in the presence and absence of electrochemically activated sulfate." *Chem. Eng. J.*, **330**, 1265 (2017).
28. Y. Yi, G. Weinberg, M. Prenzel, M. Greiner, S. Heumann, S. Becker, and R. Schlögl, "Electrochemical corrosion of a glassy carbon electrode." *Catal. Today*, **295**, 32 (2017).
29. I. Georgieva, M. Kersten, and D. Tunega, "Molecular modeling of MCPA herbicide adsorption by goethite (110) surface in dependence of pH." *Theor. Chem. Acc.*, **139**, 132 (2020).
30. E. Laviron, "General expression of the linear potential sweep voltammogram in the case of diffusionless electrochemical systems." *J. Electroanal. Chem.*, **101**, 19 (1979).
31. E. Mazzotta and C. Malitesta, "Electrochemical detection of the toxic organohalide 2,4-DB using a Co-porphyrin based electrosynthesized molecularly imprinted polymer." *Sensors Actuators, B Chem.*, **148**, 186 (2010).
32. T. A. Enache and A. M. Oliveira-Brett, "Phenol and para-substituted phenols electrochemical oxidation pathways." *J. Electroanal. Chem.*, **655**, 9 (2011).